Optical properties of polycrystalline diamond films in the far-infrared

A. J. Gatesman, R. H. Giles†, J. Waldman

University of Lowell
Department of Physics
Lowell, MA 01854

L. P. Bourget, R. Post

ASTeX®
Applied Science and Technology, Inc.
Woburn, MA 01801

Abstract

Room temperature Fourier transform spectroscopic transmissivity data in the far-infrared (10 - 360 cm^{-1}) were used to derive a model for the complex refractive index (n - ik) of polycrystalline diamond films grown by microwave plasma enhanced chemical vapor deposition. Transmission measurements were also made at a frequency of 19.5 cm^{-1} utilizing a CO_2 optically pumped submillimeter laser. Due to their polycrystalline nature, the diamond films exhibited a surface roughness with crystallite sizes ranging from 2 - 8 μm. This roughness introduced a diffuse scattering loss at the shorter wavelengths and is accounted for in the determination of the optical properties of the diamond. Residual absorption, proportional to λ^2, is observed at longer wavelengths ($1/\lambda < 100$ cm^{-1}).

1. Introduction

Recent studies of diamond grown by low pressure techniques have shown that they possess many of the same unique properties as natural diamond. These findings have spurred interest in the growth and production of high quality diamond films for a variety of electrical and optical applications. Potential uses for vapor grown diamond include optical coatings and windows, heat sinks for high power electronics, abrasives and wear resistant coatings. At least one important application for diamond films in the far-infrared and millimeter wavelength regions is their use as windows in gyrotron tubes. These microwave and millimeter wave generators can produce high output powers of pulsed (GW) or CW (MW) radiation. One of the design problems in scaling gyrotrons to higher power levels and shorter wavelengths is transmitting such high power through an output window. Traditionally, ceramics such as Aluminum Oxide (Al_2O_3), Beryllium Oxide (BeO) and sapphire have been used.[1] The excellent thermal conductivity[2] and anticipated low absorption in the far-infrared makes synthetic diamond a promising candidate for such windows. This study was aimed at determining the refractive index n, and extinction coefficient k, of synthetically grown polycrystalline diamond in the far-infrared and verifying the anticipated low absorption.

†University of Lowell Research Foundation, Lowell, MA 01854

2. Growth Technique and Film Characterization

The diamond films[3] studied in this research were grown on Si substrates by the method of microwave plasma enhanced chemical vapor deposition (MPCVD).[4] Prior to deposition, the silicon substrates were polished with diamond powder of 1/4 μm size to increase diamond nucleation during deposition. The substrates were then positioned in the lower portion of a microwave discharge on an inductively heated graphite stage. A closed-loop temperature control system regulates the surface temperature at the substrate through a thermocouple embedded in the stage. Typical deposition conditions are shown in Table I and gave growth rates of approximately 0.5 - 1.0 μm/hr.

Table I
Deposition Conditions Used for Synthesis of Diamond Films

Base Pressure	50 mTorr
Deposition Pressure	50 Torr
Substrate Temperature	875 - 950 C
Hydrogen Flow	250 - 500 sccm
Methane Flow	2 - 5 sccm
% Methane	0.8 - 1.0 %
Microwave power	1500 Watts
Deposition Time	10 - 140 hours

The diamond films were studied by scanning electron microscopy (SEM), optical microscopy, Raman Spectroscopy and Fourier Transform Spectroscopy. SEM micrographs (Figure 1) provided details of the film's surface and uniformity, while micrographs of the cross section were useful in studying the film's growth morphology. It was determined from these micrographs that crystallite sizes ranged from 2 - 8 μm. Utilizing an image shearing optical microscope, accurate thickness measurements were made by examining the film's cross section.

Raman spectroscopy is a structure sensitive tool which displays aspects of a material's vibrational properties and can be related to atomic bonding configurations. Since the CVD techniques are carried out in a region where graphite is thermodynamically stable, there exists the possibility of co-depositing other forms of non-diamond carbon. Raman spectroscopy, sensitive to the bonding configurations of diamond (sp^3) and graphitic carbon (sp^2) bonds, is widely used as an identification method for the vapor grown carbon materials. Figure 2 shows the Raman spectrum[5] of sample "a" used in this study. The sharp peak at 1332 cm^{-1} identifies the cubic carbon (diamond) structure and the wide peak centered around 1550 cm^{-1} is identified with graphitic carbon.[6] The spectrum is indicative of a high quality CVD diamond film.[7]

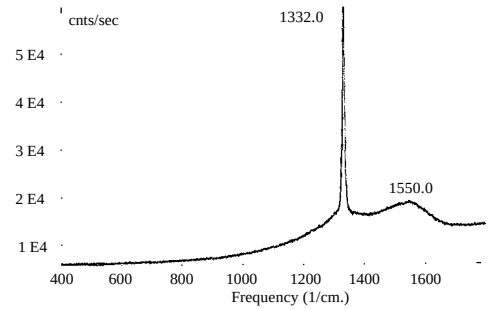

Figure 1 SEM micrograph of polycrystalline diamond sample "a"

Figure 2 Raman spectra of polycrystalline diamond sample "a"

3. Far-Infrared Spectroscopy (FTIR)

The diamond's far-infrared optical properties were studied using a Digilab FTS-80 Fourier Transform Spectrometer. The spectrometer is a Michelson type interferometer employing a mercury arc-lamp source and a mylar beamsplitter. A liquid helium cooled Si bolometer was used as the detector. Transmission measurements performed on a 76.2 μm film are shown in Figure 3. Transmission measurements were also performed at 19.49 cm^{-1} (513.1 μm) utilizing a CW CO_2 optically pumped submillimeter laser. Given the improved signal to noise ratio of the monochromatic laser source over the lower intensity broadbanded spectrometer signal, these laser measurements provided a calibration for the spectrometer's intensity scale. The laser output was created by pumping a HOOH (formic acid) gas filled cavity with a 9.23 micron (R28) CO_2 line. The CO_2 laser output was approximately 75 watts at this line and the far-infrared output power approximately five milliwatts.

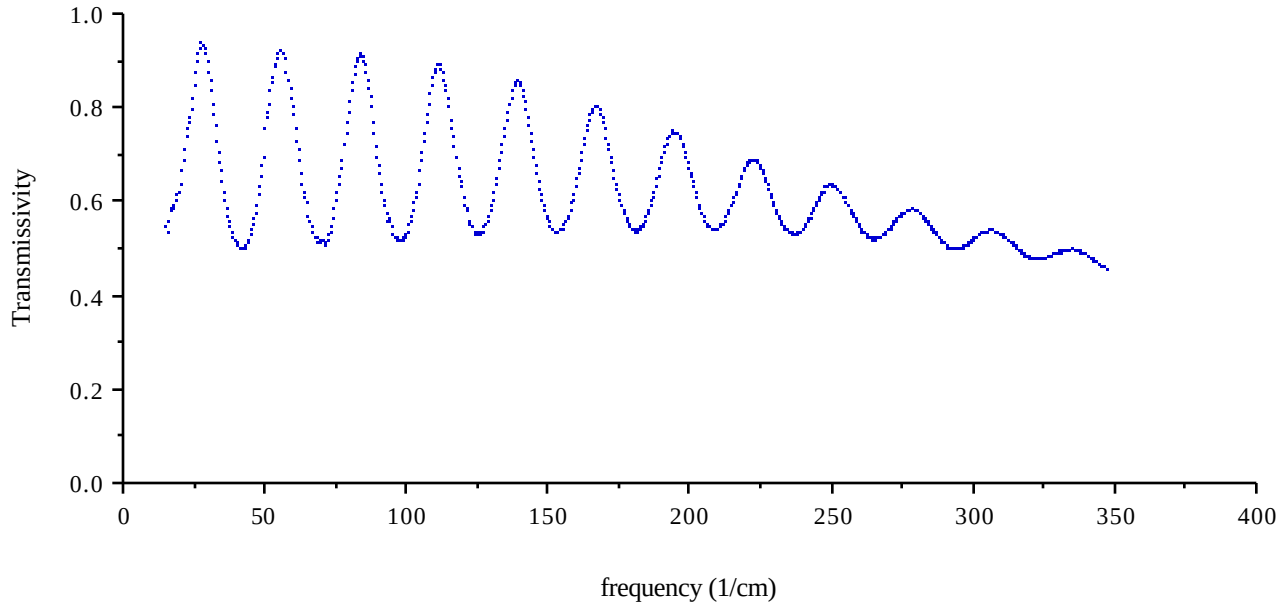

Figure 3 FTIR transmissivity data of sample "a" as a function of frequency.

To simplify analysis of the far-infrared measurements, the central region of the diamond's silicon substrate was etched with a mixture of hydrofloric, nitric and acetic acids (3:3:1) resulting in a free standing diamond film. Interference between multiple, internally reflected beams leads to a series of maxima and minima in the transmission spectrum whose intensity and location in frequency depend upon the film's refractive index and thickness. For wavelengths large compared to the rms surface roughness, specular transmission is anticipated and any loss exhibited by the transmission spectrum is associated with absorption within the deposited material itself. The rapid decline in intensity of the maxima at higher frequencies is attributed to the effects of scattering loss and not to broadband absorption of the material. Determination of the material's optical properties, in particular the diamond's extinction coefficient k, requires understanding of this influence on the FTIR data.

4. Optical Properties

Constructive interference will occur between amplitudes T_1 and T_2 (Figure 4) when their optical path difference equals an integer number of wavelengths within the material:

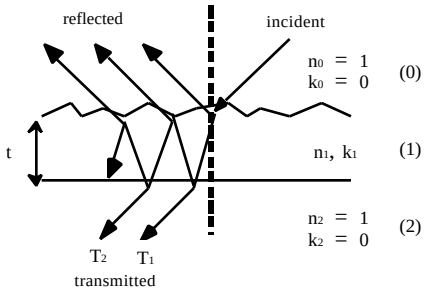

Figure 4 Schematic of free standing diamond film with rough surface showing multiple internal reflections.

$$2\,t = m\,\lambda / n$$

where t is the film thickness, λ is the vacuum wavelength, m is the order number and n is the refractive index. Solving for n,

$$n = \frac{m}{2\,t\,\nu}$$

where ν is the frequency in wavenumbers ($1/\lambda$) of the maxima. Values of the real part of the refractive index could then be calculated from the FTIR data. The uncertainty in n is due primarily to the uncertainty in the film's thickness (± 1 μm) and the limited resolution of the spectrometer (0.5 cm^{-1}). It was found that n was roughly constant in this wavelength region and had the value:

$$n = 2.36 \pm 0.02$$

The effects of surface roughness on optical spectra has been studied by many authors. Davies[8] derives a wavelength-dependent exponential term which when incorporated into the Fresnel equations, can be used to explain observed reflectivity in the regime $\lambda >> \sigma$ where σ is the rms height of the surface irregularities. Filinski[9] generalizes this work and applies a similar term to the transmission through a rough surface. The Fresnel equations were modified as follows:

$$r'_{01} = r_{01}\,\exp\left[-2\left(\frac{S}{\lambda}\right)^2 (n_0)^2\right] \qquad t'_{01} = t_{01}\,\exp\left[-\frac{1}{2}\left(\frac{S}{\lambda}\right)^2 (n_1 - n_0)^2\right]$$

$$r'_{10} = r_{10}\,\exp\left[-2\left(\frac{S}{\lambda}\right)^2 (n_1)^2\right] \qquad t'_{10} = t_{10}\,\exp\left[-\frac{1}{2}\left(\frac{S}{\lambda}\right)^2 (n_0 - n_1)^2\right]$$

$$S = 2\,\pi\,\sigma$$

The terms r_{01}, t_{01}, r_{10} and t_{10} are the smooth surface Fresnel coefficients. The lower surface, which was in contact with the Si substrate, was assumed smooth at these wavelengths so that coefficients r_{12} and t_{12} remain unchanged. Scattering losses are known to be wavelength-dependent and assumed to be dominant over true material losses at the higher frequencies (>200 cm^{-1}). Given the value of n previously calculated by analyzing the fringe locations and using k = 0, a value of σ was adjusted such that the modelled transmission matched the experimental values

at the high frequency end of the FTIR data. The effect of scattering on the entire spectrum was then assessed. To model the FTIR data, the following expression for transmission through an etalon was used:

$$\text{Transmission} = \left| \frac{t'_{01}\, t'_{12} \exp[-i\,\beta]}{1 + r'_{01}\, r'_{12} \exp[-2\,i\,\beta]} \right|^2 \qquad \text{where} \quad \beta = \frac{2\,\pi\,(n - i\,k)\,t}{\lambda}.$$

An original model consisted of a constant value of n = 2.36, σ = 2.1 μm and k set to 0 and is plotted in Figure 5, below. These parameters were found to model the FTIR data (within 2%) except for a serious discrepancy which worsened with wavelength for frequencies < 100 cm^{-1}.

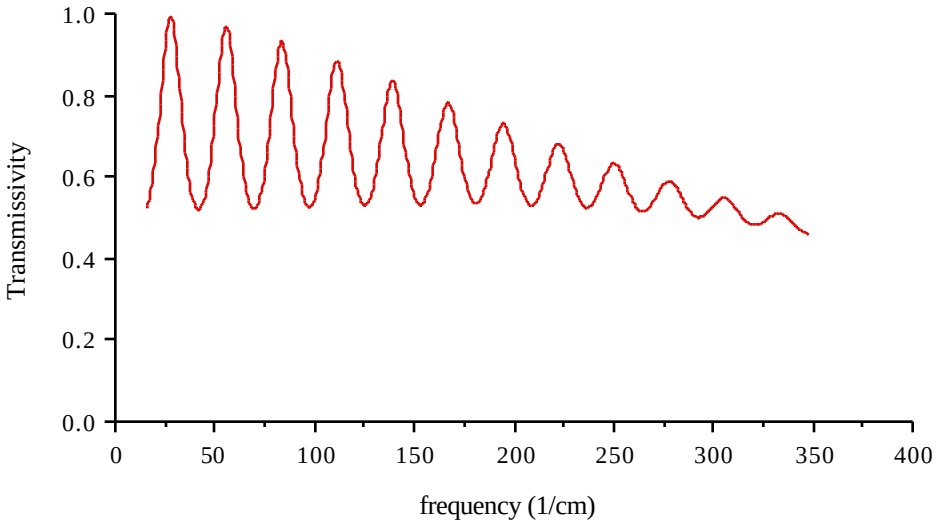

Figure 5 Rough surface model for diamond sample "a" with n = 2.36, σ = 2.1 μm and k = 0.

The rough surface model above predicts < 1% scattering loss at the long wavelengths whereas FTIR data (Figure 3) indicate maxima reaching only 94% at long wavelengths. This discrepancy indicated the presence of detectable far-infrared absorption in the diamond. One possible source of this loss at long wavelengths is the absorption due to the presence of the graphite (free carriers) in the sample.

5. Far-Infrared Free Carrier Absorption in Diamond

The classical model of free-carrier absorption is derived from the complex permittivity in the Drude theory. The relation between a material's complex refractive index and permittivity is given by:[10]

$$(n - i\,k)^2 = \varepsilon(\omega) = \varepsilon_0 + \frac{i\,4\,\pi\,N\,e^2}{m\,\omega\,(\gamma - i\,\omega)}$$

where ε_0 is the contribution to the complex dielectric constant due to the bound electrons and the second term is the contribution due to the free electrons.

$$\text{Thus} \qquad k = \frac{\varepsilon_0 \omega_p^2 \gamma}{2 n \omega(\omega^2 + \gamma^2)}.$$

$$\text{For the case } \omega >> \gamma : \quad k = \frac{\varepsilon_0 \omega_p^2 \gamma}{16 \pi^3 n c^3} \lambda^3$$

$$\text{where } \omega_p^2 = \frac{4 \pi N e^2}{m \varepsilon_0}$$

and the absorption coefficient $\alpha = 4\pi k/\lambda$ has the expected λ^2 dependence. Rather than α proportional to λ^2, the wavelength dependence is typically found in experiment to be λ^n where $1 < n < 3$.[11] A wavelength-dependent extinction coefficient given by $k = \beta \lambda^2$, where β was an adjustable parameter, was found to best fit the FTIR data. The final parameters used to model the data were $n = 2.36$, $\sigma = 2.1$ μm and $k = 15 \lambda^2$, with λ in cm. These derived parameters were used to calculate the modelled transmissivity shown in Figure 6 below along with the FTIR data. The model is seen to agree quite well over the entire frequency range studied.

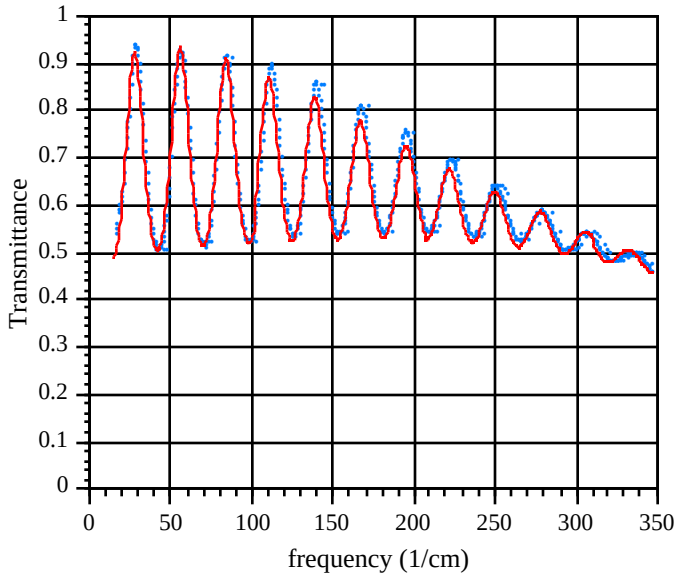

Figure 6 FTIR transmissivity data (points) and model (solid line) of diamond sample "a" for $n = 2.36$, $\sigma = 2.1$ μm and $k = 15\lambda^2$.

6. Discussion

Several other diamond samples (thicknesses 10 - 20 μm) were studied and gave similiar results to those described above. However only sample "a", which was by far the thickest, provided unambigious evidence of far-infrared absorption.

Present optical data can be found for diamond in the ultra-violet to infrared regions.[12,13,14] However no index data can be found for diamond (natural or synthetic) in the far-infrared. Edwards and Ochoa[15] have measured the refractive index n for natural type IIa diamond in the infrared from 400 - 4000 cm^{-1} (25 μm - 2.5 μm) and fitted the data to a Hertzberger type dispersion formula described in their paper. Their infrared values join smoothly with the known visible data. Figure 7 plots the values of n calculated in this study and shows reasonable agreement with the literature.

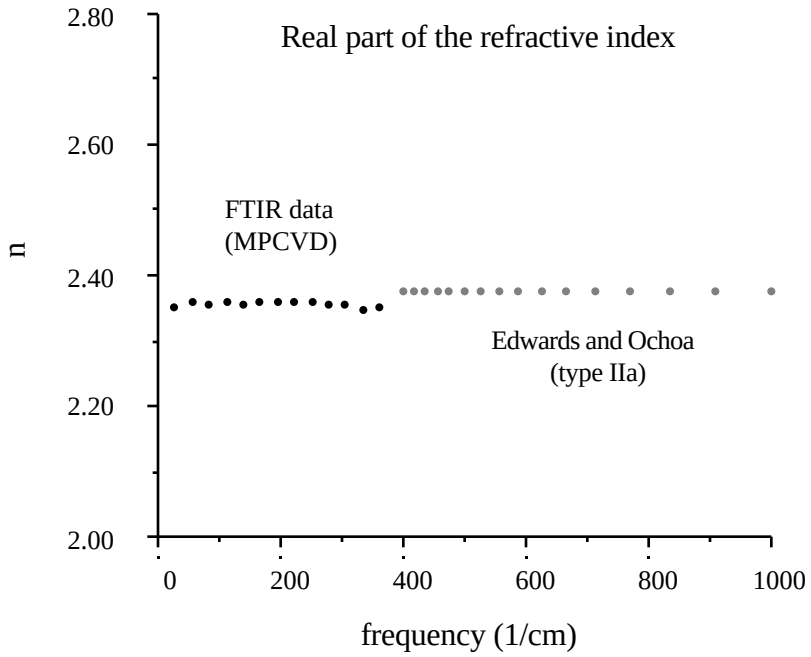

Figure 7 FTIR index values plotted versus frequency. Also plotted is the data from ref. 15 on natural diamond.

Uncertainty in the diamond's extinction coefficient depends critically on the transmissivity level of the FTIR data. In transmission type measurements, FTIR data were reproducible to within 1 - 2%. This small uncertainty in T has a relatively large effect on the precision of k (approximately 20%). However, what is of interest is the *behavior* of k as a function of frequency. k was seen to increase with λ and thus imply, as described in Section 5, some type of free carrier absorption of the far-infrared radiation. Afsar gives accurate data on the absorption of various high power laser window materials.[16] He reports absorption coefficients for Beryllia (BeO) and Alumina 995 which are one order of magnitude lower than this paper calculates for CVD diamond. Furthermore, the Beryllia and Alumina 995 data indicate *decreasing* absorption with wavelength whereas the absorption in CVD diamond was shown to increases with wavelength in the far-infrared. This long wavelength absorption may limit the applicability of currently available CVD diamond for use as a low loss window material.

7. Conclusion

A far-infrared (10 - 360 cm^{-1}) spectroscopic study of polycrystalline diamond films grown by MPCVD allowed for the calculation of the material's complex refractive index (n - ik). Calculated values of n exhibit no detectable dispersion and match with known infrared data on natural diamond. The as-grown diamond surface exhibited a surface roughness which had a predictable effect on the FTIR data at higher frequencies (> 100 cm-1). The simple model used to explain transmission through a rough surface predicted a rms surface irregularity height of 2.1 μm which is consistent with the diamond crystallite sizes (2 - 8 μm) determined through microscopy. The incorporated graphitic carbon shown in the Raman spectrum may explain the free carriers predicted by the material's frequency dependence of k and is one possible explaination of the far-infrared loss at long wavelengths.

8. References

1. H. Jory, K. Felch, E. Jongewaard, "Material Requirements for Gyrotron Windows," IEEE digest, pp. 302-303 Jan. 1987

2. D. T. Morelli, C. P. Beetz, and T. A. Perry, "Thermal Conductivity of Diamond Films," J. Appl. Phys. 64 (6), 15 Sept. 1988

3. Diamond samples were grown and provided by ASTeX®, Applied Science and Technology, Inc., Woburn, MA 01801

4. An excellent introduction to the synthesis of MPCVD diamond is given by:

   Koji Kobashi, Kozo Nishimura, Yoshio Kawate, and Takefumi Horiuchi, "Synthesis of Diamonds by use of Microwave Plasma Chemical-Vapor Deposition: Morphology and Growth of Diamond Films," Phy. Rev. B 38(6) 1988

5. Raman spectroscopy of diamond sample "a" was provided by Diane Knight, Materials Research Laboratory, The Pennsylvania State University

6. Diane S. Knight and William B. White, "Raman and Fluorescence Spectroscopic Characterization of Diamonds and CVD Diamond Films," SPIE Vol. 1055 pp. 144-151 Raman Scattering, Luminescence, and Spectroscopic Instrumentation in Technology, (1989)

7. Diane S. Knight and William B. White, "Characterization of Diamond Films by Raman Spectroscopy," J. Mater. Res., Vol. 4, No. 2, pp. 385-393, Mar/Apr 1989

8. H. Davies, "The Reflection of Electromagnetic Waves from a Rough Surface," Proc. I.E.E., Pt.III, 101, 209-214 (1954)

9. I. Filinski, "The Effects of Sample Imperfections on Optical Spectra," Phys. Stat. Sol. (b) 49, 577 (1972)

10. J. D. Jackson, Classical Electrodynamics, 2nd ed. Chap. 7, John Wiley and Sons, 1975

11. E. D. Palik and R. T. Holm, Optical Characterization of Semiconductors, Chap. 7, pp. 324-329

12. D. L. Windt et al, "Optical Constants for Thin Films of C, Diamond, Al, Si and CVD SiC from 24 Å to 1216 Å," Appl. Opt. 27, 2 (1988)

13. E. D. Palik, Handbook of Optical Constants of Solids, E. D. Palik, Ed. (Academic, Orlando, 1985)

14. H. R. Phillip and E. A. Taft, "Optical Properties of Diamond in the Vacuum Ultraviolet," Phys. Rev. 127, 159 (1962)

15. D. F. Edwards and E. Ochoa, "Infrared Refractive Index of Diamond," JOSA Letters, Vol. 71, No. 5, May 1981

16. M. N. Afsar and K. J. Button, "Millimeter and Submillimeter Wave Measurements of Complex Optical and Dielectric Parameters of Materials: I. 2.5 mm to 0.66 mm for Alumina 995, Beryllia, Fused Silica, Borosilicate and Glass ceramic, "International Journal of Infrared and Millimeter Waves," Vol. 2, No. 5, Sept. 1981